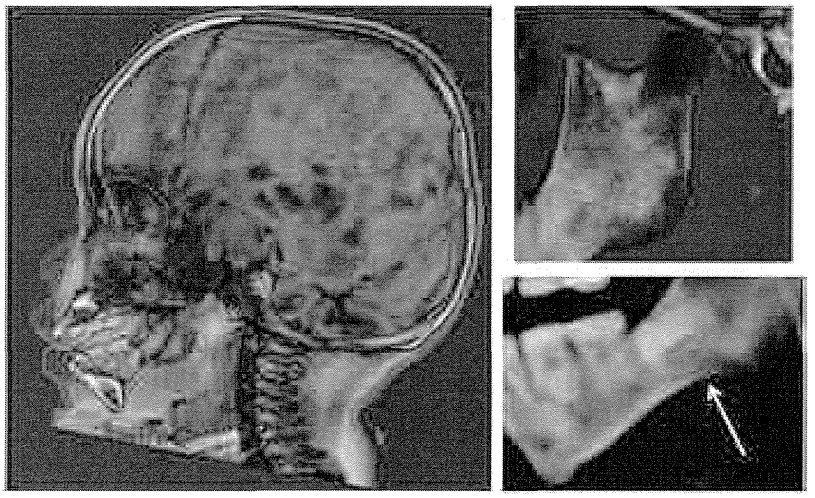

Fig. 4 Multi-detector row computed tomography (MDCT)-synthesized lateral radiograph (left) and close view of mandible (right) of Patient 3 at age of 6 years. Note the macrocephalic skull with hypoplastic facial bones (left). Mandibular anomalies are also noted, characterized by thick and flat head of the condylar process, short condylar neck, narrow mandibular notch (right upper) and antegonial notching (right lower).

Table 5 Lateral cephalometric analysis with MDCT of four patients

Patient	1	2	3	4
Skeletal				
Convexity	7.85	3.47	5.29	0.50
A-B plane	−0.12	−0.95	−1.78	0.76
SNA	4.06	−1.78	−1.78	−1.21
SNB	0.42	−2.89	−2.61	−1.14
Facial angle	−1.39	−1.54	1.39	0.53
SNP	−1.14	−2.99	−3.13	−1.56
Y axis	0.00	−0.15	−0.45	−0.84
SN-S·Gn	0.06	1.68	3.29	1.40
Mandibular plane	1.18	0.00	0.74	0.94
Gonial angle	0.77	−1.23	0.29	0.93
GZN	−0.12	2.33	2.51	2.09
FH to SN	−0.38	1.97	3.98	2.16
Dental				
U-1 to FH plane	2.37	−2.62	−0.31	4.44
U-1 to SN plane	3.12	−1.10	−2.41	3.02
L-1 to mandibular	1.17	4.94	−1.88	−1.28
Interincisal	−3.04	−2.04	0.80	−2.41
Occlusal plane	2.36	1.17	−0.69	−1.23

Unit, S.D.

cast studies are often difficult to perform, especially in the infantile period when patients tend to show marked irritability. MDCT is a useful tool for precise evaluation of craniofacial and oral manifestations in multiple congenital anomaly/intellectual disability syndromes (Hirai et al. 2011).

In conclusion, characteristic craniofacial and oral features frequently noted in patients with Costello syndrome might be true/relative macrocephaly with facial bone hypoplasia, gingival hypertrophy, malocclusion, occlusal attrition, small dental arches, microdontia, and convex face. Craniofacial and dental abnormalities are common in Costello syndrome patients and comprehensive dental care should be provided from early infancy.

ACKNOWLEDGMENTS

The authors are grateful to Professor Takahide Maeda for his helpful advice. We also thank Dr Kensuke Matsune, Dr Kenji Shimizu, Dr Yasuo Takahashi, and Hitoshi Yabe for their invaluable assistance. This study was funded in part by a Grant for the Support of Projects for Strategic Research at Private Universities by the Ministry of Education, Culture, Sports, Science and Technology (MEXT; 2008–2012), and by a grant from the Ministry of Health, Labour and Welfare, Japan.

REFERENCES

Abe Y, Aoki Y, Kuriyama S et al. 2012. Prevalence and clinical features of Costello syndrome and cardio-facio-cutaneous syndrome in Japan: findings from a nationwide epidemiological survey. Am J Med Genet A 158A:1083–1094.

Aoki Y, Niihori T, Kawame H et al. 2005. Germline mutations in HRAS proto-oncogene cause Costello syndrome. Nat Genet 37:1038–1040.

Becker MH, Coccaro PJ, Converse JM. 1976. Antegonial notching of the mandible: an often overlooked mandibular deformity in congenital and acquired disorders. Radiology 121:149–151.

Delrue MA, Chateil JF, Arveiler B, Lacombe D. 2003. Costello syndrome and neurological abnormalities. Am J Med Genet A 123A:301–305.

Der Kaloustian VM, Moroz B, McIntosh N, Watters AK, Blaichman S. 1991. Costello syndrome. Am J Med Genet 41:69–73.

Di Rocco M, Gatti R, Gandullia P, Barabino A, Picco P, Borrone C. 1993. Report on two patients with Costello syndrome and sialuria. Am J Med Genet 47:1135–1140.

van Eeghen AM, van Gelderen I, Hennekam RC. 1999. Costello syndrome: report and review. Am J Med Genet 82:187–193.

Fukawa A. 2008. Orthodontic consideration of quadruplets, compared to themselves and their parent at dento-maxilla-faical form. J Jpn Assoc Orthod 19:21–29.

Goodwin AF, Oberoi S, Landan M et al. 2012. Craniofacial and dental development in cardio-facio-cutaneous syndrome: the importance of ras signaling homeostasis. Clin Genet Sep 4. doi: 10.1111/cge.12005. [Epub ahead of print].

Hennekam RC. 2003. Costello syndrome: an overview. Am J Med Genet C Semin Med Genet 117C:42–48.
Hirai N, Yamauchi T, Matsune K et al. 2010. A comparison between two dimensional and three dimensional cephalometry on lateral radiographs and multi detector row computed tomography scans of human skulls. Int J Oral Med Sci 9:101–107.
Hirai N, Matsune K, Ohashi H. 2011. Craniofacial and oral features of Sotos syndrome: differences in patients with submicroscopic deletion and mutation of NSD1 gene. Am J Med Genet A 155A:2933–2939.
Iizuka T, Ishikawa F. 1957. Normal standards for various cephalometric analysis in Japanese adults. Nippon Kyosei Shika Gakkai Zasshi 16:4–12.
Johnson JP, Golabi M, Norton ME et al. 1998. Costello syndrome: phenotype, natural history, differential diagnosis, and possible cause. J Pediatr 133:441–448.
Kato K. 1979. [Studies on growth and development of dentition in Japanese children – examination of the longitudinal casts from deciduous dentition of 3-year-old to permanent dentition (author's transl)]. Shika Gakuho 79:991–1027. (In Japanese.)
Kawame H, Matsui M, Kurosawa K et al. 2003. Further delineation of the behavioral and neurologic features in Costello syndrome. Am J Med Genet A 118A:8–14.
Otsubo J. 1964. A longitudinal study of dental development between 6–13 years of age: growth changes of dentition. Nippon Kyosei Shika Gakkai Zasshi 23:182–190.
Rauen KA, Schoyer L, McCormick F et al. 2010. Proceedings from the 2009 genetic syndromes of the Ras/MAPK pathway: from bedside to bench and back. Am J Med Genet A 152A:4–24.
Teebi AS, Shaabani IS. 1993. Further delineation of Costello syndrome. Am J Med Genet 47:166–168.
Yamauchi T, Hirai N, Matsune K et al. 2010. Accuracy of tooth development stage, tooth size and dental arch width in multi detector row computed tomography scans of human skulls. Int J Oral Med Sci 9:108–114.
Zampino G, Mastroiacovo P, Ricci R et al. 1993. Costello syndrome: further clinical delineation, natural history, genetic definition, and nosology. Am J Med Genet 47:176–183.

RESEARCH ARTICLE

AMERICAN JOURNAL OF medical genetics

Craniofacial and Oral Features of Sotos Syndrome: Differences in Patients With Submicroscopic Deletion and Mutation of *NSD1* Gene

Norimitsu Hirai,[1]* Kensuke Matsune,[2] and Hirofumi Ohashi[3]

[1]Department of Pediatric Dentistry, Nihon University Graduate School of Dentistry at Matsudo, Chiba, Japan

[2]Department of Pediatric Dentistry, Nihon University School of Dentistry at Matsudo, Chiba, Japan

[3]Division of Medical Genetics, Saitama Children's Medical Center, Saitama, Japan

Received 7 October 2010; Accepted 22 January 2011

Sotos syndrome is a well-known overgrowth syndrome caused by haploinsufficiency of *NSD1* gene located at 5q35. There are two types of mutations that cause *NSD1* haploinsufficiency: mutations within the *NSD1* gene (mutation type) and a 5q35 submicroscopic deletion encompassing the entire *NSD1* gene (deletion type). We investigated detailed craniofacial, dental, and oral findings in five patients with deletion type, and three patients with mutation type Sotos syndrome. All eight patients had a high palate, excessive tooth wear, crowding, and all but one patient had hypodontia and deep bite. Hypodontia was exclusively observed in the second premolars, and there were no differences between the deletion and mutation types in the number of missing teeth. Another feature frequently seen in common with both types was maxillary recession. Findings were more frequently and more pronounced in deletion type than in mutation type included mandibular recession, scissors or posterior cross bite, and small dental arch with labioclination of the maxillary central incisors. It is noteworthy that although either scissors bite or crossbite was present in all of the deletion-type patients, neither of these was observed in mutation-type patients. Other features seen in a few patients include enamel hypoplasia (two deletion patients), and ectopic tooth eruption (one deletion and one mutation patients). Our study suggests that Sotos syndrome patients should be observed closely for possible dental and oral complications especially for malocclusion in the deletion type patients. © 2011 Wiley Periodicals, Inc.

Key words: Sotos syndrome; *NSD1*; submicroscopic deletion; small dental arch; malocclusion; mandibular recession

How to Cite this Article:
Hirai N, Matsune K, Ohashi H. 2011. Craniofacial and oral features of Sotos syndrome: differences in patients with submicroscopic deletion and mutation of *NSD1* gene.
Am J Med Genet Part A 155:2933–2939.

INTRODUCTION

Sotos syndrome is a congenital genetic disorder characterized by overgrowth starting before birth, specific facial manifestations (macrocephaly, prominent forehead, hypertelorism, downslanting palpebral fissures, and pointed chin), advanced bone age, and developmental impairment. Since its initial description by Sotos et al. [1964] several hundred patients have been reported to date. It may be accompanied by a variety of complications, including cardiovascular, urinogenital, and ophthalmic malformations, skeletal abnormalities, and seizures. Dental and oral findings have been reported to include premature tooth eruption, hypodontia, enamel hypoplasia, excessive tooth wear, maxillary and mandibular recession, talon cusps, fused teeth, and expanded pulp cavity of deciduous teeth [Welbury and Fletcher, 1988; Cole and Hughes, 1994; Inokuchi et al., 2001; Gomes-Silva et al., 2006; Takei et al., 2007; Nishimura et al., 2008].

Kurotaki et al. [2002] reported that this syndrome is caused by haploinsufficiency of the *NSD1* nuclear receptor SET domain containing protein 1 gene located on 5q35. There are two main types that cause *NSD1* haploinsufficiency: mutations within the *NSD1* gene, and a submicroscopic deletion in the region that contains the *NSD1* gene (constant deletion of approximately 2.2 Mb including *NSD1* and around 20 neighboring genes) [Kurotaki et al., 2002]. Nagai et al. [2003] investigated differences in clinical manifestations between these two types, and reported

Grant sponsor: Ministry of Education, Culture, Sports, Science and Technology (MEXT); Grant number: 2008-2012; Grant sponsor: Ministry of Health, Labour and Welfare, Japan.

*Correspondence to
Norimitsu Hirai, Department of Pediatric Dentistry, Nihon University Graduate School of Dentistry at Matsudo, 2-870-1 Sakaecho-Nishi, Matsudo, Chiba 271-8587, Japan. E-mail: hirai.norimitsu@nihon-u.ac.jp

Published online 19 October 2011 in Wiley Online Library (wileyonlinelibrary.com)
DOI 10.1002/ajmg.a.33969

that major anomalies such as central nervous, cardiovascular, and urinogenital abnormalities are more common in the deletion-type. Their only reference to dental findings, however, stated that early tooth eruption occurred in both types with no significant difference.

The first detailed investigation of dental and oral findings seen in Sotos syndrome based on *NSD1* genetic diagnosis was carried out by Kotilainen et al. [2009]. They analyzed dental and oral findings from 13 patients with Sotos syndrome (all except one with the mutation type), including panoramic imaging, and reported the characteristic oral complications of Sotos syndrome, including hypodontia of the second premolars. We here report on the results of our investigation of detailed craniofacial, dental, and oral findings in five patients with deletion-type, and three patients with mutation-type Sotos syndrome.

MATERIALS AND METHODS

Patients

The eight patients comprised a group who underwent examination at Saitama Children's Medical Center. Five patients (three males, two females; age, 6–13 years) were identified as having a submicroscopic deletion on 5q35 including the *NSD1* gene, and three (all females; age, 6–10 years) were identified as having a mutation of the *NSD1* gene. Deletions were identified by fluorescence in situ hybridization (FISH) analysis of metaphase chromosomes from peripheral blood, using a total of seven bacterial artificial chromosome (BAC) clones comprising the BAC clone that includes the *NSD1* gene (RP11-99N22) together with those toward the centromere (RP11-880A16, RP11-690I8, RP11-991B23) and toward the telomere (RP11-147K7, RP11-452O4, and RP11-158F10). The results showed that the same ~2 Mb deletion was present in all five patients. Mutation analysis using genomic DNA extracted from peripheral blood was performed by polymerase chain reaction (PCR) and direct sequencing of all translated regions for exon 2–23. The results identified mutations generating premature termination in both Patients 6 and 7, comprising a five base deletion (2053–2057delAAGTA) and a base deletion (5431delC), respectively, and a missense mutation (4991G>C) in Patient 8. Details of clinical manifestations are shown in Table I. This study protocol was approved by the Ethics Committee of Saitama Children's Medical Center and proper informed consents were obtained from the legal guardians of the patients.

Oral and Dental Studies

Physical examination and dental cast studies were used to evaluate palatal morphology, tooth calcification, dental arches, occlusion, tooth size, and tooth eruption status. Panoramic and lateral cephalometric radiographs reconstructed from multi-detector row computed tomography (MDCT) were also used to evaluate the relationship of craniofacial, dental and skeletal structures, and hypodontia [Hirai et al., 2010; Yamauchi et al., 2010]. Crown and

TABLE I. Clinical Manifestations of Eight Patients With Sotos Syndrome

	Deletion type patients					Mutation type patients		
	1	2	3	4	5	6	7	8
Gender	M	F	F	M	M	F	F	F
Ages (years)	7	8	6	7	13	7	10	6
Overgrowth	–	–	–	–	–	+	+	+
Intellectual disability	Moderate	Moderate	Moderate	Moderate	Moderate	Mild	–	Mild
Seizure	–	+	–	+	–	–	+	–
Craniofacial features								
Macrocephaly	+	+	+	–	+	+	+	–
Prominent forehead	+	+	+	+	+	+	+	–
Hypertelorism	+	+	+	+	+	+	+	+
Downslanting palpebral fissures	+	+	+	+	+	+	+	+
Pointed chin	+	+	+	+	+	+	+	+
Strabismus	+	+	+	–	–	+	–	–
Skeletal anomaly								
Scoliosis	–	–	–	+	+	–	+	+
Pes planovalgus	+	–	+	+	+	+	–	+
Cardiovascular anomaly	AR	PDA	–	PDA, ASD, VSD	–	VSD, CoA	MR	–
Urogenital anomaly	Hydronephrosis, VUR	–	–	–	–	Urethrocele	Hydronephrosis, hydroureter	–
Others	Hearing loss	Myelomeningocele, umbilical hernia	–	–	–	–	–	–

M, male; F, female; AR, aortic regurgitation; PDA, patent ductus arteriosus; ASD, atrial septal defect; VSD, ventricular septal defect; CoA, coarctation of aorta; MR, mitral regurgitation; VUR, vesicoureteral reflux; +, present; –, absent.

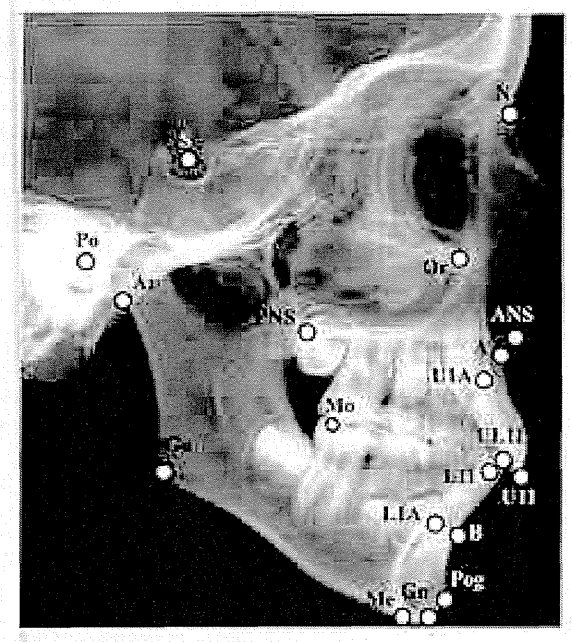

FIG. 1. Landmark points, angles, and lines used in cephalometric analysis and profilogram. Landmarks: N, nasion; Or, orbitale; S, sella turcia; Po, porion; Ar, articulare; Go, gonion; Me, menton; Gn, gnathion; Pog, pogonion; A, A-point; B, B-point; ANS, anterior nasal spine; Mo, molar occlusion; U1A, upper central incisor root apex; U1I, upper central incisor edge; L1A, lower central incisor root apex; L1I, lower central incisor edge; UL1I, middle of U1I and L1I. Angles: convexity, N-A line to the A-Pog line; A-B plane, N-Pog line to the A-B line; SNA, S-N line to the N-A line; SNB, S-N line to the N-B line; facial angle, Po-Or line to the N-Pog line; SNP, S-N line to the N-Pog line; y-axis, Po-Or line to the S-Gn line; SN-S-Gn, S-N line to the S-Gn line; mandibular plane, Po-Or line to the Me-the lower border of the mandible line; gonial angle, Ar-the posterior border of the ramus of the mandible line to the Me-the lower border of the mandible line; GZN, S-N line to the Ar-the posterior border of the ramus of the mandible line; FH to SN, Po-or line to the S-N line; U-1 to FH plane, U1I-U1A line to the Po-or line; U-1 to SN plane, U1I-U1A line to the S-N line; L-1 to mandibular, L1I-L1A line to the Me-the lower border of the mandible; interincisal, U1I-U1A line to the L1I-L1A line; occlusal plane, Po-Or line to the Mo-UL1I line.

dental arch sizes were measured using a caliper with a resolution accuracy of 0.01 mm. Lateral cephalometric analysis was performed based on the method developed by Iizuka and Ishikawa [1957] (Fig. 1). All data in this study (tooth size, dental arch form size, and cephalometric findings) were compared with standard values for Japanese individuals [Otsubo, 1957; Otsubo et al., 1964].

RESULTS

Oral and dental anomalies noted in eight patients are summarized in Table II. All eight patients had a high palate, crowding, and excessive tooth wear. All but one (Patient 1 with *NSD1* deletion) had hypodontia exclusively in the second premolars. There were no differences between the deletion-type and mutation-types in the number of missing teeth (mean number of missing teeth was 2 in the deletion-type and 2.6 in the mutation-type) (Fig. 2). The results of cephalometric analysis showed that among the five deletion-type patients, maxillary and mandibular recession was present in three and maxillary recession alone in one, whereas among the three mutation-type patients maxillary and mandibular recession was present in one and maxillary recession alone in one. The deletion-type was regarded as having a stronger tendency for mandibular recession (Table III). In terms of occlusion, crowding was present in all patients, and deep bite was seen in all but one (Patient 2 with *NSD1* deletion). It is noteworthy that although either scissors bite (Patients 1, 3, and 4) or cross bite (Patients 2 and 5) was present in all of the deletion-type patients, neither of these was observed in mutation-type patients (Fig. 3).

Small dental arch was present in all the deletion-type patients and one mutation-type patient (Table IV). In terms of morphological categories of small dental arch, the maxilla exhibited a narrow dental arch with labioclination of the central incisors in all five deletion-type patients, with the mandible being saddle-shaped in three patients and U-shaped in two, while the mutation-type patient had U-shaped upper and lower dental arches (Fig. 4). In terms of tooth size, both microdontia and macrodontia were occasionally seen in both the deletion-type and mutation-types, but no characteristic findings were present in either type (data not shown). Enamel hypoplasia was present in two out of the five deletion-type patients (Patients 2 and 5), but was not present in the mutation-type. In addition, ectopic eruption of the first molar was present in one deletion-type patient (Patient 4, right mandibular) and one mutation-type patient (Patient 6, bilateral maxillary). Some representative photographs of oral and dental anomalies noted in patients studied are shown in Figure 5.

DISCUSSION

The oral manifestations observed in common with both deletion and mutation type Sotos syndrome patients noted here were a high palate, excessive tooth wear, recession of maxilla, deep bite, crowding, and hypodontia. Hypodontia has been previously described by several authors [Inokuchi et al., 2001; Callman et al., 2006; Gomes-Silva et al., 2006; Nishimura et al., 2008]. Kotilainen et al. [2009] recently investigated 13 patients with Sotos syndrome (12 patients with *NSD1* mutations and one with *NSD1* deletion) and found one or more premolar teeth were absent in 9 out of 13 patients (8 out of 12 mutation patients and one deletion-type patient). Based on the observation that the deletion patient had the most severe phenotype of tooth agenesis, involving not only the second premolars and the third molars, but also one mandibular incisor, they noted the possibility that patient with the *NSD1* deletion had the most severe tooth agenesis. In our study, however, which included five deletion-type patients, although similar high rates of hypodontia were observed in both the deletion-type and mutation-type, we did not observe any difference in severity in either the deletion-type or mutation-type.

One noteworthy difference between the deletion-type and mutation-type was the fact that either scissors bite or cross bite

TABLE II. Oral and Dental Anomalies in Ogre Patients

	Deletion type patients					Mutation type patients			Total	
Oral anomalies	1	2	3	4	5	6	7	8	Deletion type	Mutation type
High palate	+	+	+	+	+	+	+	+	5/5	3/3
Excessive tooth wear	+	+	+	+	+	+	+	+	5/5	3/3
Hypodontia	−	+	+	+	+	+	+	+	4/5	3/3
Maxillary recession	+	−	+	+	+	+	+	−	4/5	2/3
Mandibular recession	−	−	+	+	+	−	+	−	3/5	1/3
Malocclusion										
Scissors bite	+	−	+	+	−	−	−	−	3/5	0/3
Cross bite	−	+	−	−	+	−	−	−	2/5	0/3
Deep bite	+	−	+	+	+	+	+	+	4/5	3/3
Crowding	+	+	+	+	+	+	+	+	5/5	3/3
Small dental arch	+	+	+	+	+	−	+	−	5/5	1/3
Maxilla	N	N	N	N	N	U	U	U		
Mandibula	S	U	S	S	U	U	U	U		
Labioclination of maxillary central incisor	+	+	+	+	+	−	−	−	5/5	0/3
Enamel hypoplasia	−	+	+	−	−	−	−	−	2/5	0/3
Ectopic tooth eruption	−	−	−	+	−	+	−	−	1/5	1/3

N, narrow dental arch; U, U-shaped dental arch; S, saddle-shaped dental arch. +, present; −, absent.

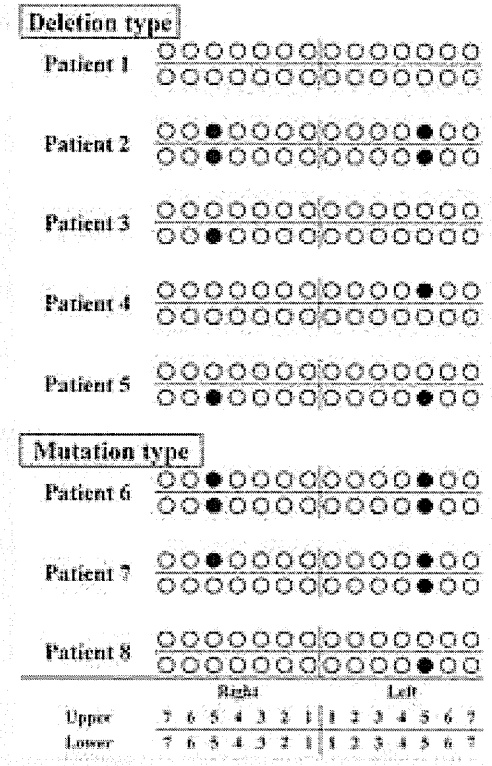

FIG. 2. Hypodontia in eight patients with Sotos syndrome. ●, Congenitally missing teeth.

was observed in all deletion-type patients, whereas neither was present in the mutation-type. All of the deletion-type patients had small dental arches, and in terms of morphological categories, the maxilla exhibited a narrow dental arch with labioclination of the central incisors in all five deletion-type patients, with the mandible being saddle-shaped in three patients and U-shaped in two. Only one single mutation-type patient had small dental arches with both upper and lower dental arches being U-shaped. Narrowing of the dental arch is more pronounced in the narrow-shape and saddle-shape compared with the U-shape. It is possible that the degree of narrowing of the dental arch in the deletion-type and the misalignment in arch morphology between the maxilla and mandible causes scissors bite or cross bite.

In addition, maxillary and mandibular recession has also been reported as a dental manifestation of Sotos syndrome [Welbury and Fletcher, 1988; Takei et al., 2007]. In our results, there was a tendency toward maxillary and mandibular recession in the deletion-type and maxillary recession in the mutation-type. Based on these findings, there was a tendency for maxillary recession to occur in both the deletion-type and mutation-type, but there was also a tendency toward the occurrence of mandibular recession in the deletion-type. Taken in conjunction with the pronounced mandibular recession seen in the deletion-type on cephalometric analysis, mandibular malformations, including those of the dental arch, may be regarded as characteristic of the deletion-type. The cause is unknown, but in the deletion-type, minute genomic imbalances, involving considerable number of genes other than the *NSD1* gene, may either: (1) directly cause deficient growth of the mandibular area; or (2) secondarily cause malocclusion or abnormal dental arch morphology as a result of dysfunction of the perioral muscles associated with more

TABLE III. Lateral Cephalometric Analysis With MDCT of Eight Patients

	Deletion type patients					Mutation type patients		
	1	2	3	4	5	6	7	8
Skeletal								
Convexity	−2.56	−1.05	−0.66	−1.80	−1.95	−4.56	−2.52	−2.94
A–B plane	−1.12	−3.96	1.68	−0.32	1.40	2.15	1.96	2.56
SNA	−2.54	1.24	−2.28	−3.45	−2.32	−2.69	−3.18	−1.63
SNB	−1.80	1.71	−3.31	−3.18	−2.84	−0.76	−2.29	−0.07
Facial angle	0.68	−3.23	−0.47	0.38	0.34	0.38	−1.55	1.43
SNP	−0.71	1.77	−1.76	−1.16	−0.63	0.02	−2.22	0.11
Y-axis	−0.50	−0.37	−0.38	−0.09	0.17	−0.36	1.29	−1.34
SN-S-Gn	3.08	−1.30	0.32	3.86	0.93	0.22	1.86	−0.30
Mandibular plane	1.29	1.05	−1.47	0.30	1.12	−0.58	1.98	−0.29
Gonial angle	6.24	−0.15	−4.06	−5.27	0.73	0.29	0.44	3.06
GZN	0.77	0.09	3.01	2.84	1.19	−0.37	1.52	−0.27
FH to SN	2.38	−1.15	0.71	2.55	0.98	0.52	0.97	1.37
Denture								
U-1 to FH plane	1.30	1.37	2.94	0.30	0.72	−0.47	0.50	0.69
U-1 to SN plane	0.51	1.87	2.56	−0.52	0.24	−0.64	−0.46	0.21
L-1 to mandibular	−2.24	−0.47	0.98	−1.47	−1.64	−2.39	−0.46	−1.93
Interincisal	−0.07	−1.07	−1.53	0.46	0.22	1.90	−0.83	0.71
Occlusal plane	−0.99	1.09	−0.76	−0.24	2.97	−1.37	1.35	−0.49

Unit: SD.

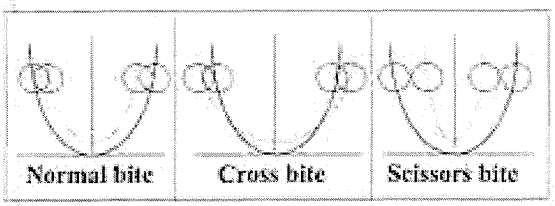

FIG. 3. Schematic representations of normal and abnormal occlusions. ——, Maxillary dental arch; – – – –, mandibular dental arch; ◯, maxillary first molar; ◌, mandibular first molar.

pronounced developmental impairment [Grabowski et al., 2007a,b; Stahl et al., 2007].

Enamel hypoplasia has also been reported as a dental manifestation of Sotos syndrome [Imokuchi et al., 2001]. Kotilainen et al. [2009] reported enamel hypoplasia in four out of 13 patients (all mutation type). In our study, enamel hypoplasia was present in two out of five deletion-type patients, but not in any mutation-type patients. Enamel hypoplasia is thought to be a common manifestation that can occasionally occur in both the deletion-type and mutation-type rather than a manifestation that is prone to occur in either type.

As mild to moderate intellectual disability is common in Sotos syndrome, conventional panoramic and cephalometric studies

TABLE IV. Dental Arch Measurements in Eight Patients

	Deletion type patients					Mutation type patients		
	1	2	3	4	5	6	7	8
Maxillary								
W_c	−0.55	Deciduous	0.04	Deciduous	1.79	−1.75	0.61	−1.38
W_m	−3.76	−3.59	0.02	−4.18	−3.11	−1.73	−2.04	−1.76
$L_{1/1}$	2.68	1.33	2.68	1.02	−0.69	1.44	0.14	−1.36
Mandibular								
W_c	Deciduous	Deciduous	−1.00	Deciduous	−0.73	−1.81	−2.70	−0.30
W_m	−4.82	−2.51	−2.16	−4.45	−3.38	−1.57	−4.34	0.96
$L_{1/1}$	0.81	1.32	1.85	0.63	−3.40	0.20	−2.07	0.56

Unit: SD.

The W_c and W_m represent the distance between the primary cuspids (the canines), and the first molars, respectively. The $L_{1/1}$ represents the length from the mesial surface of the first molars to central point of incisors.

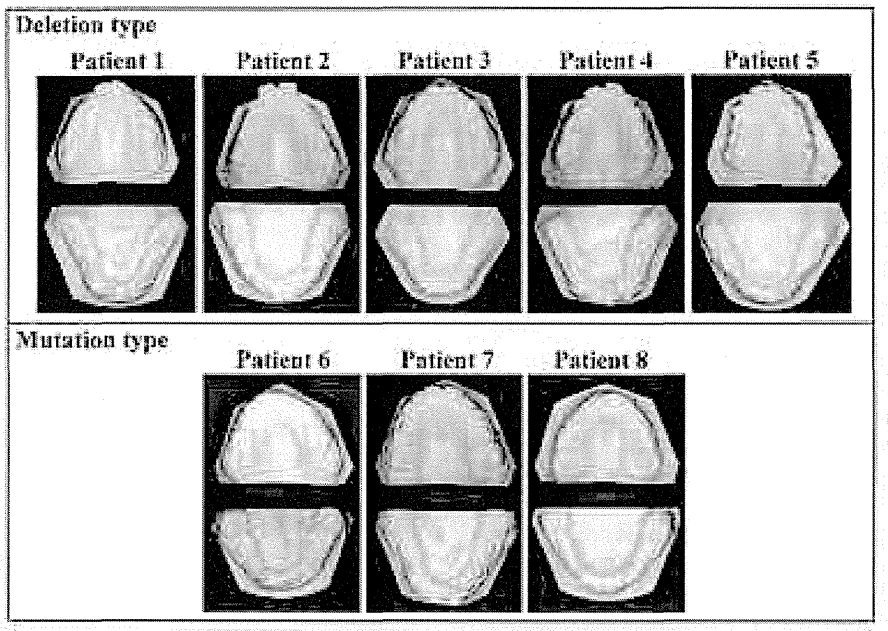

FIG. 4. Dental arch shapes of eight patients. Upper panel: maxillary dental casts, lower panel: mandibular dental casts. A narrow maxillary dental arch with labioclination of the central incisors is noted in all five deletion type patients, with the mandibula being saddle-shaped in three patients (Patients 1, 3, and 4) and U-shaped in two (Patients 2 and 5), while U-shaped upper and lower dental arches are noted in all three mutation-type patients (Patients 6, 7, and 8).

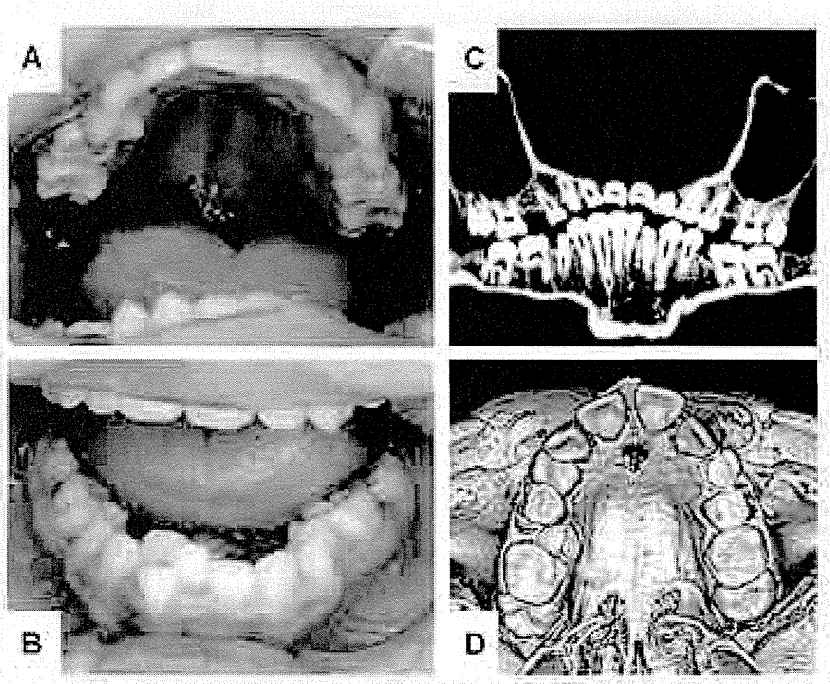

FIG. 5. Oral photographs (A,B) and MDCT-synthesized panoramic radiograph (C) of Patient 7 at age of 10 years and MDCT-synthesized upper dental arch of Patient 6 at age of 7 years (D). Note: high palate, malocclusion, small dental arch, excessive tooth wear (A,B), missing upper second premolars on both side and lower left second premolar (C), ectopic tooth eruption of first molars on both side (D).

were often difficult to perform in childhood. Thus, in this study, MDCT was used as a substitute for cephalometric radiographs and panoramic radiographs, and by which maxillofacial manifestations could be accurately evaluated [Hirai et al., 2010; Yamauchi et al., 2010].

In view of oral and dental management, we would like to provide recommendations as follows: periodic dental check up to prevent dental caries or gingivitis should be started early after one or more deciduous teeth have erupted. Around age 7 years, detailed oral and dental evaluations, including dental cast studies and MDCT, is recommended for possible hypodontia and malocclusion. If the patient has hypodontia, preceding deciduous tooth (teeth) should be maintained as long as possible with proper care. Although malocclusion like scissors bite and cross bite requires early treatment, including expansion of upper or lower jaw, to prevent craniofacial disabilities such as facial asymmetry and temporomandibular joint dysfunction, the treatment should be carefully decided based on consideration of capability of cooperation of the patients.

In conclusion, features seen more frequently and more pronounced form in deletion-type than in mutation-type were small dental arch with labioclination of the maxillary central incisors, mandibular recession, and scissors or posterior cross bite. Sotos syndrome patients should be followed closely for possible dental and oral complications especially for malocclusion in the deletion-type.

ACKNOWLEDGMENTS

The authors are grateful to Prof. Takahide Maeda for his helpful advice. We also thank to Dr. Kenji Shimizu, Dr. Yasuo Takahashi, and Hitoshi Yabe for their invaluable assistance. This study was funded in part by a Grant for the Support of Projects for Strategic Research at Private Universities by the Ministry of Education, Culture, Sports, Science and Technology (MEXT; 2008-2012), and by a grant from the Ministry of Health, Labour and Welfare, Japan.

REFERENCES

Cullinan AP, Anand P, Sheehy EC. 2006. Sotos syndrome with hypodontia. Inter J Paediatri Dent 16:143–146.

Cole TRP, Hughes HE. 1994. Sotos syndrome: A study of the diagnostic criteria and natural history. J Med Genet 31:20–32.

Gomes-Silva JM, Ruviere DB, Segatto RA, de Queiroz AM, de Freitas AC. 2006. Sotos syndrome: A case report. Spec Care Dentist 26:257–262.

Grabowski R, Kundt G, Stahl F. 2007a. Interrelation between occlusal findings and orofacial myofunctional status in primary and mixed dentition: Part III: Interrelation between malocclusions and orofacial dysfunctions. J Orofac Orthop 68:462–476.

Grabowski R, Stahl F, Gaebel M, Kundt G. 2007b. Relationship between occlusal findings and orofacial myofunctional status in primary and mixed dentition. Part I: Prevalence of malocclusions. J Orofac Orthop 68:26–37.

Hirai N, Yamauchi T, Matsune K, Kobayashi R, Yabe H, Ohashi H, Maeda T. 2010. A comparison between two dimensional and three dimensional cephalometry on lateral radiographs and multi detector row computed tomography scans of human skulls. Int J Oral-Med Sci 9:101–107.

Iizuka T, Ishikawa F. 1957. Normal standards for various cephalometric analysis in Japanese adults. Nippon Kyosei Shika Gakkai Zasshi 16:4–12.

Isokuchi M, Nomura J, Mitsumura Y, Sekida M, Tagawa T. 2001. Sotos syndrome with enamel hypoplasia: A case report. J Clin Pediatr Dent 25:313–316.

Kotilainen J, Pohjola P, Pirinen S, Arte S, Nieminen P. 2009. Premolar hypodontia is a common feature in Sotos syndrome with a mutation in the NSD1 gene. Am J Med Genet Part A 149A:2409–2414.

Kurotaki N, Imaizumi K, Harada N, Masuno M, Kondoh T, Nagai T, Ohashi H, Naritomi K, Tsukahara M, Makita Y, Sugimoto T, Sonoda T, Hasegawa T, Chinen Y, Tomita HH, Kinoshita A, Yoshiura KK, Ohta T, Kishino T, Fukushima Y, Niikawa N, Matsumoto N. 2002. Haploinsufficiency of NSD1 causes Sotos syndrome. Nat Genet 30:365–366.

Nagai T, Matsumoto N, Kurotaki N, Harada N, Niikawa N, Ogata T, Imaizumi K, Kurosawa K, Kondoh T, Ohashi H, Tsukahara M, Makita Y, Sugimoto T, Sonoda T, Yokoyama T, Uetake K, Sakazume S, Fukushima Y, Naritomi K. 2003. Sotos syndrome and haploinsufficiency of NSD1: Clinical features of intragenic mutations and submicroscopic deletions. J Med Genet 40:289–289.

Nishimura K, Mori Y, Yamauchi M, Kamakura N, Homma H, Nomura H, Miyamoto E, Matsumoto M, Shintani S, Ooshima T. 2008. Sotos syndrome with oligodontia: A case report. Pediatric Dent J 18:187–191.

Otsuka J. 1957. A study on the tooth material in Japanese adults of normal occlusion, its relationship to coronal and basal arches. Nippon Kyosei Shika Gakkai Zasshi 16:36–46.

Otsuka J, Ishikawa F, Kuwahara Y. 1964. A longitudinal study of dental development between 6–13 years of age: Growth changes of dentition. Nippon Kyosei Shika Gakkai Zasshi 23:182–190.

Sotos IF, Dodge PR, Muirhead D, Crawford JD, Talbot NB. 1964. Cerebral gigantism in childhood. A syndrome of excessively rapid growth with acromegalic features and a nonprogressive neurologic disorder. N Engl J Med 271:109–116.

Stahl F, Grabowski R, Gaebel M, Kundt G. 2007. Relationship between occlusal findings and orofacial myofunctional status in primary and mixed dentition. Part II: Prevalence of orofacial dysfunctions. J Orofac Orthop 68:374–90.

Takei K, Suzuki K, Yamaguchi H, Ohtawa Y. 2007. Dentofacial growth in patients with Sotos syndrome. Bull Tokyo Dent Coll 48:73–85.

Welbury RR, Fletcher HI. 1988. Cerebral gigantism (Sotos syndrome) two case reports. J Paediatr Dent 4:41–44.

Yamauchi T, Hirai N, Matsune K, Kobayashi R, Yabe H, Ohashi H, Maeda T. 2010. Accuracy of tooth development stage, tooth size and dental arch width in multi detector row computed tomography scans of human skulls. Int J Oral Med Sci 9:108–114.

Mutations in *B3GALT6*, which Encodes a Glycosaminoglycan Linker Region Enzyme, Cause a Spectrum of Skeletal and Connective Tissue Disorders

Masahiro Nakajima,[1,21] Shuji Mizumoto,[2,21] Noriko Miyake,[3,21] Ryo Kogawa,[2] Aritoshi Iida,[1] Hironori Ito,[4] Hiroshi Kitoh,[5] Aya Hirayama,[6] Hiroshi Mitsubuchi,[7] Osamu Miyazaki,[8] Rika Kosaki,[9] Reiko Horikawa,[10] Angeline Lai,[11] Roberto Mendoza-Londono,[12] Lucie Dupuis,[12] David Chitayat,[12] Andrew Howard,[13] Gabriela F. Leal,[14] Denise Cavalcanti,[15] Yoshinori Tsurusaki,[3] Hirotomo Saitsu,[3] Shigehiko Watanabe,[16] Ekkehart Lausch,[17] Sheila Unger,[18] Luisa Bonafé,[19] Hirofumi Ohashi,[16] Andrea Superti-Furga,[19] Naomichi Matsumoto,[3] Kazuyuki Sugahara,[2] Gen Nishimura,[20] and Shiro Ikegawa[1,*]

Proteoglycans (PGs) are a major component of the extracellular matrix in many tissues and function as structural and regulatory molecules. PGs are composed of core proteins and glycosaminoglycan (GAG) side chains. The biosynthesis of GAGs starts with the linker region that consists of four sugar residues and is followed by repeating disaccharide units. By exome sequencing, we found that *B3GALT6* encoding an enzyme involved in the biosynthesis of the GAG linker region is responsible for a severe skeletal dysplasia, spondyloepimetaphyseal dysplasia with joint laxity type 1 (SEMD-JL1). *B3GALT6* loss-of-function mutations were found in individuals with SEMD-JL1 from seven families. In a subsequent candidate gene study based on the phenotypic similarity, we found that *B3GALT6* is also responsible for a connective tissue disease, Ehlers-Danlos syndrome (progeroid form). Recessive loss-of-function mutations in *B3GALT6* result in a spectrum of disorders affecting a broad range of skeletal and connective tissues characterized by lax skin, muscle hypotonia, joint dislocation, and spinal deformity. The pleiotropic phenotypes of the disorders indicate that *B3GALT6* plays a critical role in a wide range of biological processes in various tissues, including skin, bone, cartilage, tendon, and ligament.

Skeletal dysplasias represent a vast collection of genetic disorders of the skeleton, currently divided into 40 groups.[1] Spondyloepimetaphyseal dysplasia (SEMD) is one group (group 13) of skeletal dysplasia that contains more than a dozen distinctive diseases. SEMD with joint laxity (SEMD-JL) is a subgroup of SEMD that consists of type 1 (SEMD-JL1 [MIM 271640]) and type 2 (SEMD-JL2 [MIM 603546]). SEMD-JL1 or SEMD-JL Beighton type is an autosomal-recessive disorder that shows mild craniofacial dysmorphism (prominent eye, blue sclera, long upper lip, small mandible with cleft palate) and spatulate finger with short nail.[2] The large joints of individuals with SEMD-JL1 are variably affected with hip dislocation, elbow contracture secondary to radial head dislocation, and clubfeet. Joint laxity is particularly prominent in the hands. Skeletal changes of SEMD-JL1 are characterized by moderate platyspondyly with anterior projection of the vertebral bodies, hypoplastic ilia, and mild metaphyseal flaring.[3] Kyphoscoliosis progresses with age, leading to a short trunk, whereas platyspondyly become less conspicuous and the vertebral bodies appear squared in shape with age. Recently, dominant kinesin family member 22 (*KIF22* [MIM 603213]) mutations have been found in SEMD-JL2;[4,5] however, the genetic basis of SEMD-JL1 remains unknown.

To identify the SEMD-JL1-causing mutation, we performed whole-exome sequencing experiments. We recruited seven individuals with SEMD-JL1 from five unrelated Japanese families (F1–F5) and a Singapore/Japanese family (F6) (Table 1). One family (F1) had a pair of affected sibs (P1 and P2) from nonconsanguineous parents. Genomic DNA was extracted by standard procedures

[1]Laboratory for Bone and Joint Diseases, Center for Integrative Medical Sciences, RIKEN, Tokyo 108-8639, Japan; [2]Laboratory of Proteoglycan Signaling and Therapeutics, Frontier Research Center for Post-Genomic Science and Technology, Graduate School of Life Science, Hokkaido University, Sapporo 001-0021, Japan; [3]Department of Human Genetics, Yokohama City University Graduate School of Medicine, Yokohama 236-0004, Japan; [4]Department of Orthopaedic Surgery, Central Hospital, Aichi Prefectural Colony, Kasugai 480-0392, Japan; [5]Department of Orthopaedic Surgery, Nagoya University School of Medicine, Nagoya 466-8550, Japan; [6]Department of Pediatrics, Akita Prefectural Center on Development and Disability, Akita 010-1407, Japan; [7]Department of Neonatology, Kumamoto University Hospital, Kumamoto 860-8556, Japan; [8]Department of Radiology, National Center for Child Health and Development, Tokyo 157-8535, Japan; [9]Division of Medical Genetics, National Center for Child Health and Development, Tokyo 157-8535, Japan; [10]Division of Endocrinology and Metabolism, National Center for Child Health and Development, Tokyo 157-8535, Japan; [11]Department of Paediatric Medicine, KK Women's and Children's Hospital, Singapore 229899, Singapore; [12]Department of Paediatrics, The Hospital for Sick Children and University of Toronto, Toronto, ON M5G 1X8, Canada; [13]Department of Surgery, The Hospital for Sick Children and University of Toronto, Toronto, ON M5G 1X8, Canada; [14]The Professor Fernando Figueira Integral Medicine Institute (IMIP), Recife, PE 50070-550, Brazil; [15]Skeletal Dysplasia Group, Department of Medical Genetics, Faculty of Medical Sciences, State University of Campinas (UNICAMP), Campinas, SP 13083-970, Brazil; [16]Division of Medical Genetics, Saitama Children's Medical Center, Saitama 339-8551, Japan; [17]Division of Paediatric Genetics, Centre for Pediatrics and Adolescent Medicine, University of Freiburg, Freiburg 79106, Germany; [18]Medical Genetics Service, University of Lausanne, CHUV, Lausanne 1011, Switzerland; [19]Department of Pediatrics, University of Lausanne, CHUV, Lausanne 1011, Switzerland; [20]Department of Pediatric Imaging, Tokyo Metropolitan Children's Medical Center, Fuchu 183-8561, Japan
[21]These authors contributed equally to this work
*Correspondence: sikegawa@ims.u-tokyo.ac.jp
http://dx.doi.org/10.1016/j.ajhg.2013.04.003.

Table 1. Clinical and Radiographic Findings of the Individuals with *B3GALT6* Mutations

Subject ID	P1	P2	P3	P4	P5	P6	P7	P8	P9	P10	P11	P12
Family ID	F1	F1	F2	F3	F4	F5	F6	F7	F8	F9	F9	F10
Clinical diagnosis	SEMD-JL1	SEMD-JL1	SEMD-JL1	SEMD-JL1	SEMD-JL1	SEMD-JL1	SEMD-JL1	SEMD-JL1	EDS-PF	EDS-PF	EDS-PF	EDS-PF
General Information												
Ethnicity	Japanese	Japanese	Japanese	Japanese	Japanese	Japanese	Japanese/ Singaporean	Vietnamese	Italian	Italian/ Canadian	Italian/ Canadian	Brazilian
Gender	M	M	F	M	F	F	M	M	M	F	F	F
Age	34 years	31 years	12 years, 7 months	6 years	5 years, 1 month	12 years	2 years, 9 months	34 years	8 months	7 years	1 month	5 years, 1 month
Gestational age	39 weeks, 2 days	full term	37 weeks	40 weeks, 1 day	39 weeks, 5 days	full term	39 weeks	full term	ND	36 weeks	37 weeks	39 weeks
Birth length (cm)	ND	ND	36	ND	43.1	42	43	(average)	ND	44	44	44
Birth weight (g)	ND	2,200	2,124	2,832	2,535	2,222	2,485	3,500	ND	2,097	2,790	3,300
Clinical Features												
Height (cm) (SD)[a]	127.7 (−7.4)	130 (−7.0)	88.8 (−10.7)	94 (−4.0)	90 (−4.0)	118.4 (−5.1)	78.2 (−4.0)	118 (−9.1)	66 (−1.6)	90 (−6.8)	45 (−3.7)	81 (−5.9)
Weight (kg) (SD)[a]	40.3 (−2.2)	36.9 (−2.5)	13.2 (−3.7)	15.4 (−1.5)	14.4 (−1.3)	23.2 (−2.0)	10.6 (−1.9)	28 (−3.3)	5.65 (−3.0)	13.9 (−2.2)	2.65 (−2.8)	8.5 (−8.4)
Craniofacial												
Flat face with prominent forehead	ND	ND	+	+	+	+	+	−	+	+	+	+
Prominent eyes, proptosis	ND	ND	+	−	−	+	+	−	+	+	+	+
Blue sclerae	ND	ND	+	+	+	−	+	−	+	+	+	−
Long upper lip	ND	ND	−	+	+	−	+	+	+	+	+	−
Micrognathia	ND	ND	+	+	+	+	−	+	−	−	−	−
Cleft palate	ND	ND	−	−	−	−	−	−	−	−	−	+
Musculoskeletal												
Kyphoscoliosis[b]	+ (7 months)	+ (1.2 years)	+ (8 months)	+ (infancy)	+ (2 years)	+ (3 months)	+ (8 months)	+ (1 year)	+ (6 months)	++ (prenatal)	++ (prenatal)	++ (2 years)
Spatulate finger	−	ND	+	+	+	+	−	−	+	+	+	−
Finger laxity	ND	ND	+	+	−	−	+	−	++	+	+	+
Large joint laxity	ND	ND	+	+	−	−	+	−	++	++	++	+
Restricted elbow movement	+	ND	+	+	+	−	−	+	+	+	+	+
Hand contracture	−	−	−	−	−	+	−	−	−	+	+	−

(*Continued on next page*)

Table 1. ***Continued***

Subject ID	P1	P2	P3	P4	P5	P6	P7	P8	P9	P10	P11	P12
Hip dislocation	–	–	–	+	–	+	–	–	–	+	+	+
Clubfeet	–	–	+	–	–	–	+	–	–	+	+	–
Muscular hypotonia	–	–	+	–	–	–	–	–	++	++	++	++
Skin and Hair												
Doughy skin	ND	ND	+	–	–	–	+	–	++	+	+	+
Hyperextensibility	ND	ND	+	–	–	–	+	–	++	+	+	–
Cutis laxa	ND	ND	–	–	–	–	–	–	+	+	–	+
Sparse hair	ND	ND	–	–	–	–	–	–	+	+	+	–
Others			MR, DD				camptodactyly			DD		pectus excavatum
Radiological Features												
Platyspondyly	+[c]	+[c]	+[c]	+	+	+	+	+	+	+	+	+
Anterior beak of vertebral body[b]	+	+	– (4 years)	– (5 years)	+	+	+	–	+	+	+	+
Short ilia	+	+	+	+	+	+	+	+	+	+	+	+
Prominent lesser trochanter	+	+	+	–	+	+	+	+	+	+	+	+
Metaphyseal flaring	+	+	+	+	+	+	+	+	+	–	+	+
Epiphyseal dysplasia of femoral head	–	–	–	+	–	+	–	–	–	–	+	+
Elbow malalignment	ND	ND	+	+	+	+	+	+	+	+	+	+
Advanced carpal ossification[b]	– (9 years)	ND	– (12 years)	+	+	+	+	ND	+	– (7 years)	–	– (5 years)
Carpal fusion	ND	ND	+	–	–	–	–	–	–	–	–	–
Metacarpal shortening	ND	ND	+	+	+	+	+	+	–	–	+	–
Overtubulation	–	–	–	–	–	–	–	–	+	+	+	+

Abbreviations are as follows: SEMD-JL1, spondyloepimetaphyseal dysplasia with joint laxity type 1; EDS-PF, Ehlers-Danlos syndrome, progeroid form; ND, no data; MR, mitral regurgitation; DD, developmental delay.
[a]At last presentation.
[b]Age at medical attention provided in parentheses.
[c]Absent at age 20 years in P1 and P2 and at age 12 years in P3.

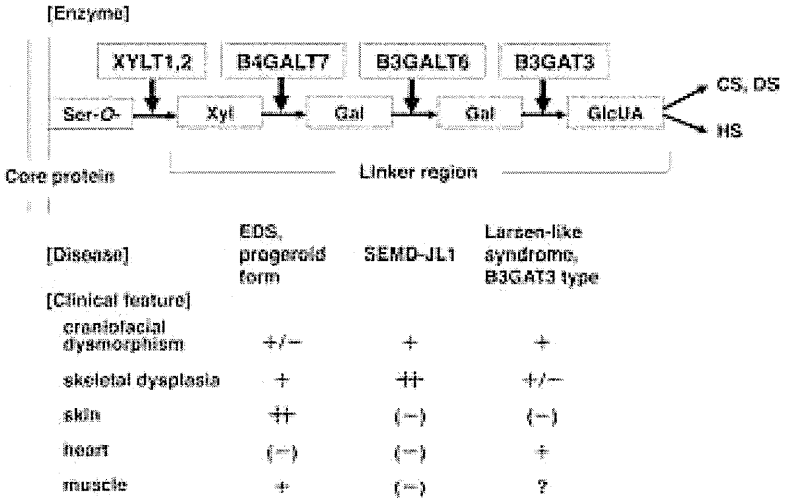

Figure 1. Enzymes Involved in Biosynthesis of the Glycosaminoglycan Linker Region and Summary Features of Diseases Caused by Their Defects Based on a Conventional Concept for the Diseases

The biosyntheses of GAGs start with the formation of a common tetrasaccharide linker sequence covalently attached to the core protein. The linker region synthesis involves a single linear pathway composed of four successive steps catalyzed by distinctive enzymes. Abbreviations are as follows: XYLT, β-xylosyltransferase; B4GALT7, xylosylprotein β1,4-galactosyltransferase, polypeptide 7 (β1,4-galactosyltransferase-I); B3GALT6, UDP-Gal, βGal β1,3-galactosyltransferase polypeptide 6 (β1,3-galactosyltransferase-II); B3GAT3, β-1,3-glucuronyltransferase 3 (glucuronosyltransferase I); Ser-*O*, the serine residue of the GAG attachment site on the proteoglycan core protein; Xyl, xylose; Gal, galactose; GlcUA, D-glucuronic acid; CS, chondroitin sulfate; DS, dermatan sulfate; HS, heparan sulfate; EDS, Ehlers-Danlos syndrome; SEMD-JL1, spondyloepimetaphyseal dysplasia with joint laxity type 1.

from peripheral blood, saliva, or Epstein-Barr virus-immortalized lymphocyte of the individuals with SEMD-JL1 and/or their parents after informed consent. The study was approved by the ethical committee of RIKEN and participating institutions. We captured the exomes of the seven subjects as previously described.[6,7] In brief, we sheared genomic DNA (3 μg) by Covaris S2 system (Covaris) and processed with a SureSelect All Exon V4 kit (Agilent Technologies). We sequenced DNAs captured by the kit with HiSeq 2000 (Illumina) with 101 base pair-end reads. We performed the image analysis and base calling by HiSeq Control Software/Real Time Analysis and CASAVA1.8.2 (Illumina) and mapped the sequences to human genome hg19 by Novoalign. We processed the aligned reads by Picard to remove PCR duplicate. The mean depth of coverage for reads was 132.8×, and, on average, 91.0% of targeted bases had sufficient coverage (20× coverage) and quality for variant calling (Table S1 available online). The variants were called by Genome Analysis Toolkit 1.5-21 (GATK) with the best practice variant detection with the GAKT v.3 and annotated by ANNOVAR (2012 February 23).

Based on the hypothesis that SEMD-JL1 is inherited in an autosomal-recessive fashion, we filtered variants with the script created by BITS (Tokyo, Japan) according to following conditions: (1) variants registered in ESP5400, (2) variants found in our in-house controls (n = 274), (3) synonymous changes, (4) rare variants registered in dbSNP build 135 (MAF < 0.01), and (5) variants associated with segmental duplication. After combining variants selected by the homozygous mutation model and the compound heterozygous mutation model, we selected genes shared by individuals from three or more families. The analysis of the next-generation sequencing identified possible compound heterozygous variants in *B3GALT6* in individuals from three families (Table S2). In addition, two other subjects had possible causal heterozygous variants of *B3GALT6*.

B3GALT6 (RefSeq accession number NM_080605.3) is a single-exon gene on chromosome 1p36.33. It encodes UDP-Gal:βGal β1,3-galactosyltransferase polypeptide 6 (or galactosyltransferase-II: GalT-II), an enzyme involved in the biosynthesis of the glycosaminoglycan (GAG) linker region.[8] The biosyntheses of dermatan sulfate (DS), chondroitin sulfate (CS), and heparin/heparan sulfate (HS) GAGs start with the formation of a tetrasaccharide linker sequence, glucuronic acid-β1-3-galactose-β1-3-galactose-β1-4-xylose-β1 (GlcUA-Gal-Gal-Xyl), which is covalently attached to the core protein. The linker region synthesis involves a single linear pathway composed of four successive steps catalyzed by distinctive enzymes (Figure 1). The first step is the addition of xylose to the hydroxy group of specific serine residues on the core protein by xylosyltransferases from UDP-Xyl, followed by two distinct galactosyltransferases (GalT-I and II) and a glucuronosyltransferase from UDP-Gal and UDP-GlcUA, respectively. The next hexosamine addition is critical because it determines which GAG (i.e., CS, DS, or HS) is assembled on the linker region. GalT-II encoded by *B3GALT6* functions in the third step of the linker formation (Figure 1).

To confirm the results obtained by the next-generation sequencing, we examined the seven subjects used for the next-generation sequencing and an additional subject from a Vietnamese family (F7) by direct sequence of the PCR products from genomic DNAs using 3730xl DNA Analyzer (Applied Biosystems). The Sanger sequencing confirmed all *B3GALT6* mutations found by the next-generation sequencing and identified additional *B3GALT6* mutations. The results indicated that *B3GALT6* mutations were found in all subjects (Tables 2 and S1). All but P4 from F3 were compound heterozygotes of missense mutations. In P4, only a heterozygous c.1A>G (p.Met1?) mutation was found, although we searched for a *B3GALT6* mutation in the entire coding region, 5′ and 3′ UTRs, and flanking

Table 2. *B3GALT6* Mutations in Spondyloepimetaphyseal Dysplasia with Joint Laxity Type 1 and Ehlers-Danlos Syndrome, Progeroid Form

Family	Clinical Diagnosis	Nucleotide Change	Amino Acid Change
F1	SEMD-JL1	c.1A>G	p.Met1?
		c.694C>T	p.Arg232Cys
F2	SEMD-JL1	c.1A>G	p.Met1?
		c.466G>A	p.Asp156Asn
F3[a]	SEMD-JL1	c.1A>G	p.Met1?
F4	SEMD-JL1	c.1A>G	p.Met1?
		c.694C>T	p.Arg232Cys
F5	SEMD-JL1	c.694C>T	p.Arg232Cys
		c.899G>C	p.Cys300Ser
F6	SEMD-JL1	c.1A>G	p.Met1?
		c.193A>G	p.Ser65Gly
F7	SEMD-JL1	c.200C>T	p.Pro67Leu
		c.694C>T	p.Arg232Cys
F8	EDS-PF	c.353delA	p.Asp118Alafs*160
		c.925T>A	p.Ser309Thr
F9	EDS-PF	c.588delG	p.Arg197Alafs*81
		c.925T>A	p.Ser309Thr
F10	EDS-PF	c.16C>T	p.Arg6Trp
		c.415_423del	p.Met139Ala141del

The nucleotide changes are shown with respect to *B3GALT6* mRNA sequence. The corresponding predicted amino acid changes are numbered from the initiating methionine residue.
[a]Only a heterozygous mutation was found.

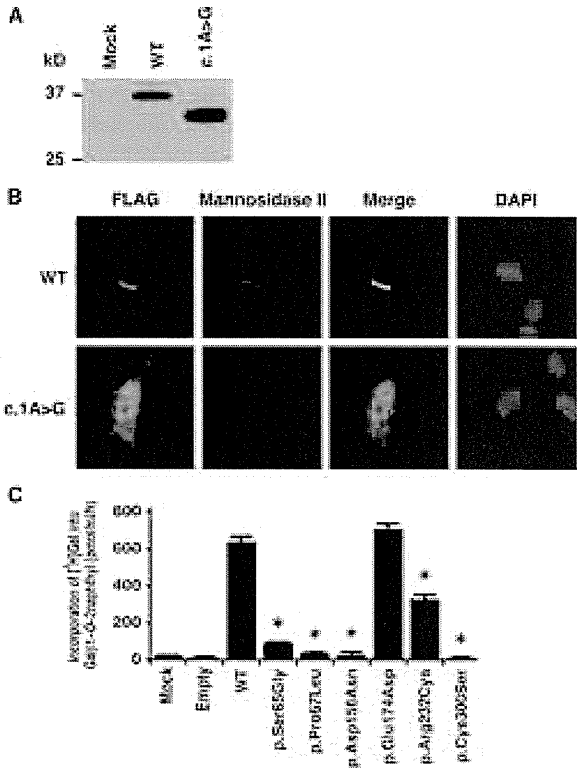

Figure 2. Analyses of B3GALT6 Missense Mutant Proteins Identified in Individuals with SEMD-JL1 In Vitro
(A) Immunoblot analysis of lysates from HeLa cells expressing transfected wild-type (WT) and mutant (c.1A>G) *B3GALT6*. The mutant *B3GALT6* yields a shortened protein. The difference of the molecular sizes between WT and mutant proteins is approximately ~4 kD.
(B) Subcellular localization of B3GALT6. HeLa cells were transfected with WT and mutant (c.1A>G) *B3GALT6*. Cells were stained with anti-FLAG (green), anti-α-mannosidase II (red), and 4′,6-diamidino-2-phenylindole (DAPI; blue). WT was expressed in the Golgi, but the mutant was found in cytoplasm and nucleus.
(C) Decreased enzyme activities of the missense mutant proteins (p.Ser65Gly, p.Pro67Lys, p.Asp156Asn, p.Arg232Cys, and p.Cys300Ser). p.Glu174Asp is a common polymorphism in the public database. The GalT-II activity is measured by incorporation of [^{3}H]Gal into Galβ1-*O*-2naphthyl (*p*mol/ml/hr) and represents the averages of three independent experiments performed in triplicate. Empty and mock indicate the GalT-II activity obtained with the conditioned medium transfected with or without an empty vector. *$p < 0.0001$ versus WT (one-way analysis of variance with Dunnett's adjustment).

regions of *B3GALT6*. Most of the mutations are predicted to be disease causing by in silico analysis. The c.1A>G (p.Met1?) mutation was found in individuals from five of the seven families.

Although mutations affecting initiation codons have been reported to be pathogenic in several diseases,[9] the effects of initiation codon mutations on the encoded protein are variable among the genes. We therefore investigated the effect of the c.1A>G (p.Met1?) mutation on the protein by using C-terminally FLAG-tagged B3GALT6 with and without the mutation expressed in HeLa cells (RIKEN Cell Bank). We detected the mutant B3GALT6 protein with a molecular weight ~4 kD lower compared with the wild-type (WT) protein (Figure 2A). These results suggest that translation initiation at the second ATG of the coding sequence, at position c.124, would become the initiation codon because of the mutation, probably resulting in an N-terminal deletion of 41 amino acids (p.Met1_Ala41del), in the same open reading frame that contains the transmembrane domain. We then examined the subcellular localization of the mutant B3GALT6 protein by immunocytochemistry. The immunofluorescence for WT-B3GALT6 was observed in a perinuclear region overlapping with that for α-mannosidase II, a marker of the Golgi as previously reported.[8] In contrast, the immunofluorescence for the mutant B3GALT6 protein was observed in the nucleus and cytoplasm (Figure 2B). Therefore, the mutant protein can be considered to be functionally null because of the mislocalization.

To investigate the causality of other *B3GALT6* missense mutations, we also examined the subcellular localization of the mutant B3GALT6 proteins by immunocytochemistry. c.193A>G (p.Ser65Gly), c.200C>T (p.Pro67Leu),

and c.694C>T (p.Arg232Cys) mutants showed mislocalization, whereas c.466G>A (p.Asp156Asn) and c.899G>C (p.Cys300Ser) mutants showed normal localization (Figure S1). To investigate whether the *B3GALT6* missense mutations affect the enzyme function, the GalT-II activities of soluble FLAG-tagged proteins for WT and mutant B3GALT6 proteins were assayed. The GalT-II activities of p.Ser65Gly-, p.Pro67Leu-, p.Asp156Asn-, p.Arg232Cys-, and p.Cys300Ser-B3GALT6 were significantly decreased compared with WT-B3GALT6 (Figure 2C), indicating that these mutations resulted in a loss of enzyme function. On the other hand, there were no significant differences in the GalT-II activities between WT-B3GALT6 and p.Glu174Asp-B3GALT6, a common polymorphism (rs12085009) in the public database (Figure 2C).

All SEMD-JL1 individuals with the *B3GALT6* mutation had the characteristic skeletal abnormalities, including platyspondyly, short ilia, and elbow malalignment (Table 1 and Figure S2); however, some had a range of extraskeletal and connective tissue abnormalities that overlapped with those seen in Ehlers-Danlos syndrome, progeroid form (EDS-PF [MIM 130070]). EDS-PF is an autosomal-recessive connective tissue disorder characterized by sparse hair, wrinkled skin, and defective wound healing with atrophic scars.[10] In addition, skeletal abnormalities so far reported in EDS-PF are limited to generalized osteopenia and radial head dislocation, which are in contrast with the severe generalized dysplasias of the axial and appendicular skeleton observed in SEMD-JL1. Thus, both disorders at first glance appear as separate clinical entities, although they share the clinical features of short stature, joint laxity and dislocation, and facial dysmorphism. In two families with individuals with EDS-PF, recessive mutations of *B4GALT7* (MIM 604327) have been found.[11,12] *B4GALT7* (RefSeq NM_007255.2) encodes an enzyme, xylosylated protein β-1,4-galactosyltransferase, that catalyzes the second step of the GAG linker region biosynthesis (Figure 1). Therefore, we speculated that B3GALT6 and B4GALT7 deficiencies might show similar phenotypes. We then examined *B3GALT6* in four additional individuals (P9–P12) who had phenotypes compatible with EDS-PF (Table 1 and Figure S3) but in whom no *B4GALT7* mutations had been found. Sanger sequencing of the EDS-PF-like subjects revealed that all were compound heterozygotes for *B3GALT6* mutations (Table 2). There were two frameshift mutations and one missense mutation (c.925T>A [p.Ser309Thr]) common in two families (F8 and F9). We investigated the enzyme function of the missense mutation by using the same assay for SEMD-JL1 missense mutations. The GalT-II activities of p.Ser309Thr-B3GALT6 were significantly decreased (Figure S4).

Collectively, 11 different mutations in individuals from 10 families were identified in *B3GALT6* by a combination of exome and targeted sequencing (Table 2 and Figure S5). None of these mutations were detected in more than 200 ethnicity-matched controls or in public databases, including the 1000 Genomes database, indicating that they are unlikely to be polymorphisms. SEMD-JL1 and EDS-PF-like individuals had no common mutations (Table 2). The individuals with *B3GALT6* mutations were short at birth and their short stature worsened with age. Their common clinical features were a flat face with prominent forehead and kyphoscoliosis (Table 1). Kyphoscoliosis was noticed in infancy in most cases and even in utero in severe cases. Although skeletal changes were essentially the same, craniofacial and skin abnormalities, joint laxities, and muscular hypotonia were variable among the individuals with *B3GALT6* mutations. Common radiographic features were platyspondyly that becomes less conspicuous with age, short ilia, and elbow malalignment (Table 1). Prominent lesser trochanters and metaphyseal flaring were seen in most cases. No individuals showed generalized osteoporosis. The disease phenotype was very variable between families (mutations), but in two familial cases, phenotypes were similar between the pair of the sibs. As a corollary, our results indicate that EDS-PF is genetically heterogeneous, with a proportion of cases being caused by mutations in *B4GALT7* and another in *B3GALT6*.

Diseases caused by defects in enzymes involved in the biosynthesis of the GAG linker region are categorized as the GAG linkeropathy. The first member of GAG linkeropathy has been identified to arise from an EDS-PF/B4GALT7 deficiency. *B4GALT7* mutations have been identified in homozygous c.808C>T (p.Arg270Cys)[12] and compound heterozygous (c.557C>A [p.Ala186Asp] and c.617T>C [p.Leu206Pro])[11] states. Another member of GAG linkeropathy manifests itself as Larsen-like syndrome, B3GAT3 type (MIM 245600). A family with individuals harboring a homozygous *B3GAT3* (MIM 606374; RefSeq NM_012200.3) mutation (c.830G>A [p.Arg227Gln]) has been identified. The clinical features of five affected individuals of the family are characterized by dislocation and laxity of joints and congenital heart defects.[11] The former considerably overlaps with the phenotypes of SEMD-JL1 and EDS-PF, two other GAG linkeropathies; however, the association of heart defects has critically differentiated this disease from the others (Figure 1).

Given that the linker region biosynthesis is nonparallel and that the defects in the three enzymes simply affect the amounts of the linker region available to form GAGs (CS, HS, DS), phenotypic similarities of the three diseases are quite understandable. The quantitative difference of the phenotypes (severity of the diseases) most probably results from the difference in the degree of enzyme defects resulting from mutations. On the other hand, qualitative differences of the three diseases (e.g., scoliosis caused by the *B3GALT6* mutation, heart disease caused by the *B3GAT3* mutation, etc.) suggest other explanations. Tissue expression patterns of the three genes do not entirely explain the differences. We examined their mRNA expression in various human tissues, including cartilage, bone, and connective tissues by quantitative real-time PCR (Figure S6). We detected strong expression of *B3GALT6* in

Table 3. The Amount of GAGs in the Lymphoblastoid Cells from Individuals with Spondyloepimetaphyseal Dysplasia with Joint Laxity Type 1

	GAG (Disaccharides/mg Acetone Powder)[a] [pmol]			
Subject	**CS/DS**	**CS**	**DS**	**HS**
Control	62	48	29	128
SEMD-JL1				
P1	313	295	118	15
P2	345	175	60	21
P3	270	162	28	20

[a]Calculated based on the peak area in chromatograms of digests with a mixture of chondroitinases ABC and AC-II (CS/DS), chondroitinases AC-I and AC-II (CS), chondroitinase B (DS), and heparinases I and III (HS).

cartilage and bone but only weak expression in skin, ligament, and tendon. *B4GALT7* expression was stronger in cartilage than *B3GALT6* and also weak in skin and ligament. *B3GAT3* expression was not specific to heart. The qualitative difference may result from the difference in the effects of the three genes on GAG formation.

To examine how *B3GALT6* mutations affects the products of GAGs in vivo, we measured the amounts of CS and HS chains at the surface of lymphoblastoid cells from the subjects by flow cytometry by using CS-stub and HS-stub antibodies as previously described.[13–15] In brief, purified GAG fractions were treated individually with a mixture of chondroitinases ABC and AC-II, a mixture of chondroitinases AC-I (EC 4.2.2.5) (Seikagaku Corp.) and AC-II (EC 4.2.2.5) (Seikagaku Corp.), chondroitinase B (EC 4.2.2.19) (IBEX Technologies), or a mixture of heparinases-I and -III (IBEX Technologies) for analyzing the disaccharide composition of CS/DS, CS, DS, and HS, respectively. The digests were labeled with a fluorophore 2-aminobenzamide (2AB) and aliquots of the 2AB derivatives of CS/DS/HS disaccharides were analyzed by anion-exchange HPLC on a PA-03 column (YMC Co.). The HS-stub antibody (3G10) showed a markedly reduced binding to the epitopes on the subjects' cells (Figure S7). The relative numbers of the HS chains presented as the mean fluorescence intensity (MFI) of the cell population stained with the antibody for P1, P2, and P3 were 26%, 56%, and 35% of the control, respectively. On the other hand, the CS-stub antibody (2B6) showed a similar binding to the epitopes on the subjects' cells relative to those of the control (Figure S7). The MFI for P1, P2, and P3 were 114%, 104%, and 106% of the control, respectively. Furthermore, we measured disaccharide of GAG chains from lymphoblastoid cells by using anion-exchange HPLC after digestion with chondroitinase and heparinase. The amounts of the disaccharide from HS chains were significantly decreased, whereas CS and DS chains were ~5 times higher than those in the control (Table 3).

Previous biochemical studies on EDS-PF with *B4GALT7* mutations show a reduction in the synthesis of DS chains.[16,17] The c.830G>A (p.Arg227Gln) mutation in *B3GAT3* causes a drastic reduction in GlcAT-I activity in fibroblasts of the individual with SEMD-JL1 and numbers of CS and HS chains on the core proteins at the surface of the fibroblasts are decreased to about half of the controls.[11] Cultured lymphoblastoid cells from individuals with a c.419C>T (p.Pro140Leu) mutation in *B3GAT3* show that defective synthesis is more pronounced for CS than for HS.[11] Taken together with our results, these findings suggest that the effects of the deficiencies of the three enzymes on GAG synthesis are not identical. A possible explanation for the qualitative phenotypic differences may be that the biosynthesis of the GAG linker region is not a simple step-by-step addition but involves parallel processing and/or alternative pathways. Other glycosyltransferases may have similar biochemical functions to these three enzymes and thus complement their deficient activities to variable degrees in cell- and/or tissue-specific manners, leading to differences in the amount of GAGs in the tissues. It is known that B3GALT6 and B4GALT7 have several homologs.[18] It must be noted that all biochemical studies so far have been performed in vitro or in cultured cells, and therefore there is a severe limitation to our understanding of the pathogenesis at tissue and organ levels.

By exome sequencing, we identified loss-of-function mutations in *B3GALT6* in 12 individuals from 10 families. The mutations produced a spectrum of connective tissue disorders characterized by lax skin, muscle hypotonia, joint dislocation, and skeletal dysplasia and deformity, which include phenotypes previously known as SEMD-JL1 and EDS-PF (Figures S1 and S2). The pleiotropic phenotypes of *B3GALT6* mutations indicate that B3GALT6 plays critical roles in development and homeostasis of various tissues, including skin, bone, cartilage, tendons, and ligaments. Biochemical studies that used lymphoblastoid cells of the individuals with *B3GALT6* mutations showed a decrease of HS and a paradoxical increase of CS and DS of the cell surface. Further clinical, genetic, and biological studies are necessary to understand the pathological mechanism of the diseases caused by enzyme defects involved in the biosynthesis of the GAG linker region and roles of the region in GAG metabolism and function.

Supplemental Data

Supplemental Data include seven figures and two tables and can be found with this article online at http://www.cell.com/AJHG/.

Acknowledgments

We thank the individuals with the disease and their family for their help to the study. We also thank the Japanese Skeletal Dysplasia Consortium. This study is supported by research grants from the Ministry of Health, Labor, and Welfare (23300101 to S.I. and N. Matsumoto; 23300201 to S.I.), by Grants-in-Aid for Young Scientists (23689052 to N. Miyake and 23790066 to S.M.) from the Japan Society for the Promotion of Science; by the Matching Program for Innovations in Future Drug Discovery and Medical Care

(K.S.); by The Ministry of Education, Culture, Sports, Science and Technology, Japan (MEXT); by a Grant-in-aid for Encouragement from the Akiyama Life Science Foundation (S.M.); by Swiss National Science Foundation Grants (31003A_141241 and 310030_132940); by The CoSMO-B project (Brazil and Switzerland); by the Leenaards Foundation (Switzerland); and by Research on intractable diseases, Health and Labour Sciences Research Grants, H23-Nanchi-Ippan-123 (S.I.).

Received: February 1, 2013
Revised: March 16, 2013
Accepted: April 5, 2013
Published: May 9, 2013

Web Resources

The URLs for data presented herein are as follows:

1000 Genomes, http://browser.1000genomes.org
ANNOVAR, http://www.openbioinformatics.org/annovar/
dbSNP, http://www.ncbi.nlm.nih.gov/projects/SNP/
GATK, http://www.broadinstitute.org/gatk/
MutationTaster, http://www.mutationtaster.org/
NHLBI Exome Sequencing Project (ESP) Exome Variant Server, http://evs.gs.washington.edu/EVS/
Novoalign, http://www.novocraft.com/main/page.php?s=novoalign
Online Mendelian Inheritance in Man (OMIM), http://www.omim.org/
Picard, http://picard.sourceforge.net/
PolyPhen, http://www.genetics.bwh.harvard.edu/pph2/
RefSeq, http://www.ncbi.nlm.nih.gov/RefSeq
SIFT, http://sift.bii.a-star.edu.sg/
UCSC Genome Browser, http://genome.ucsc.edu

References

1. Warman, M.L., Cormier-Daire, V., Hall, C., Krakow, D., Lachman, R., LeMerrer, M., Mortier, G., Mundlos, S., Nishimura, G., Rimoin, D.L., et al. (2011). Nosology and classification of genetic skeletal disorders: 2010 revision. Am. J. Med. Genet. A. *155A*, 943–968.
2. Beighton, P., Gericke, G., Kozlowski, K., and Grobler, L. (1984). The manifestations and natural history of spondylo-epimetaphyseal dysplasia with joint laxity. Clin. Genet. *26*, 308–317.
3. Nishimura, G., Satoh, M., Aihara, T., Aida, N., Yamamoto, T., and Ozono, K. (1998). A distinct subtype of "metatropic dysplasia variant" characterised by advanced carpal skeletal age and subluxation of the radial heads. Pediatr. Radiol. *28*, 120–125.
4. Boyden, E.D., Campos-Xavier, A.B., Kalamajski, S., Cameron, T.L., Suarez, P., Tanackovic, G., Andria, G., Ballhausen, D., Briggs, M.D., Hartley, C., et al. (2011). Recurrent dominant mutations affecting two adjacent residues in the motor domain of the monomeric kinesin KIF22 result in skeletal dysplasia and joint laxity. Am. J. Hum. Genet. *89*, 767–772.
5. Min, B.J., Kim, N., Chung, T., Kim, O.H., Nishimura, G., Chung, C.Y., Song, H.R., Kim, H.W., Lee, H.R., Kim, J., et al. (2011). Whole-exome sequencing identifies mutations of KIF22 in spondyloepimetaphyseal dysplasia with joint laxity, leptodactylic type. Am. J. Hum. Genet. *89*, 760–766.
6. Miyake, N., Elcioglu, N.H., Iida, A., Isguven, P., Dai, J., Murakami, N., Takamura, K., Cho, T.J., Kim, O.H., Hasegawa, T., et al. (2012). PAPSS2 mutations cause autosomal recessive brachyolmia. J. Med. Genet. *49*, 533–538.
7. Tsurusaki, Y., Okamoto, N., Ohashi, H., Kosho, T., Imai, Y., Hibi-Ko, Y., Kaname, T., Naritomi, K., Kawame, H., Wakui, K., et al. (2012). Mutations affecting components of the SWI/SNF complex cause Coffin-Siris syndrome. Nat. Genet. *44*, 376–378.
8. Bai, X., Zhou, D., Brown, J.R., Crawford, B.E., Hennet, T., and Esko, J.D. (2001). Biosynthesis of the linkage region of glycosaminoglycans: cloning and activity of galactosyltransferase II, the sixth member of the beta 1,3-galactosyltransferase family (beta 3GalT6). J. Biol. Chem. *276*, 48189–48195.
9. Saunders, C.J., Minassian, B.E., Chow, E.W., Zhao, W., and Vincent, J.B. (2009). Novel exon 1 mutations in MECP2 implicate isoform MeCP2_e1 in classical Rett syndrome. Am. J. Med. Genet. A. *149A*, 1019–1023.
10. Kresse, H., Rosthøj, S., Quentin, E., Hollmann, J., Glössl, J., Okada, S., and Tønnesen, T. (1987). Glycosaminoglycan-free small proteoglycan core protein is secreted by fibroblasts from a patient with a syndrome resembling progeroid. Am. J. Hum. Genet. *41*, 436–453.
11. Baasanjav, S., Al-Gazali, L., Hashiguchi, T., Mizumoto, S., Fischer, B., Horn, D., Seelow, D., Ali, B.R., Aziz, S.A., Langer, R., et al. (2011). Faulty initiation of proteoglycan synthesis causes cardiac and joint defects. Am. J. Hum. Genet. *89*, 15–27.
12. Faiyaz-Ul-Haque, M., Zaidi, S.H., Al-Ali, M., Al-Mureikhi, M.S., Kennedy, S., Al-Thani, G., Tsui, L.C., and Teebi, A.S. (2004). A novel missense mutation in the galactosyltransferase-I (B4GALT7) gene in a family exhibiting facioskeletal anomalies and Ehlers-Danlos syndrome resembling the progeroid type. Am. J. Med. Genet. A. *128A*, 39–45.
13. Kinoshita, A., and Sugahara, K. (1999). Microanalysis of glycosaminoglycan-derived oligosaccharides labeled with a fluorophore 2-aminobenzamide by high-performance liquid chromatography: application to disaccharide composition analysis and exosequencing of oligosaccharides. Anal. Biochem. *269*, 367–378.
14. Miyake, N., Kosho, T., Mizumoto, S., Furuichi, T., Hatamochi, A., Nagashima, Y., Arai, E., Takahashi, K., Kawamura, R., Wakui, K., et al. (2010). Loss-of-function mutations of CHST14 in a new type of Ehlers-Danlos syndrome. Hum. Mutat. *31*, 966–974.
15. Mizumoto, S., and Sugahara, K. (2012). Glycosaminoglycan chain analysis and characterization (Glycosylation/Epimerization). In Methods in Molecular Biology. In Proteoglycans: Methods and Protocols, F. Rédini, ed. (New York, USA: Humana Press, Springer), pp. 99–115.
16. Okajima, T., Fukumoto, S., Furukawa, K., and Urano, T. (1999). Molecular basis for the progeroid variant of Ehlers-Danlos syndrome. Identification and characterization of two mutations in galactosyltransferase I gene. J. Biol. Chem. *274*, 28841–28844.
17. Quentin, E., Gladen, A., Rodén, L., and Kresse, H. (1990). A genetic defect in the biosynthesis of dermatan sulfate proteoglycan: galactosyltransferase I deficiency in fibroblasts from a patient with a progeroid syndrome. Proc. Natl. Acad. Sci. USA *87*, 1342–1346.
18. Togayachi, A., Sato, T., and Narimatsu, H. (2006). Comprehensive enzymatic characterization of glycosyltransferases with a beta3GT or beta4GT motif. Methods Enzymol. *416*, 91–102.

Human Mutation
OFFICIAL JOURNAL
HGVS
HUMAN GENOME VARIATION SOCIETY
www.hgvs.org

A Response to: Loss of Dermatan-4-sulfotransferase 1 (D4ST1/CHST14) Function Represents the First Dermatan Sulfate Biosynthesis Defect, "Dermatan Sulfate-Deficient Adducted Thumb–Clubfoot Syndrome". Which Name is Appropriate, "Adducted Thumb–Clubfoot Syndrome" or "Ehlers–Danlos Syndrome"?

We thank Janecke et al. [2011] for their letter about a recently recognized dermatan 4-O-sulfotransferase 1 (D4ST1) deficiency caused by loss-of-function *CHST14* (MIM# 608429) mutations, independently found in an arthrogryposis syndrome "Adducted Thumb–Clubfoot Syndrome" (ATCS) [Dündar et al., 2009], a specific form of Ehlers-Danlos syndrome (EDS) as we have proposed (EDS, Kosho Type; EDSKT) [Miyake et al., 2010], and a subset of kyphoscoliosis type EDS without evidence of lysyl hydroxylase deficiency (EDS type VIB) coined as "Musculocontractural EDS" (MCEDS) [Malfait et al., 2010]. Janecke et al. [2011] proposed that these three conditions constitute a clinically recognizable and genetically identical type of connective tissue disorder and that the disorders should not be categorized into a form of EDS, but be termed collectively "Dermatan Sulfate-Deficient Adducted Thumb–Clubfoot Syndrome" to avoid possible confusion for both clinicians and researchers. The proposal is based on their clinical and molecular recognition of the disorder. First, the presence of multiple congenital malformations such as facial dysmorphism, cleft lip/palate, intestinal abnormalities, renal abnormalities, and features such as nephrolithiasis and muscle hypotonia in these patients are not typical in EDS, though features such as joint laxity, skin hyperextensibility/fragility, and bleeding diathesis are typical in EDS. Second, the molecular basis in the disorder is different from that in EDS.

EDS comprises a heterogeneous group of heritable connective tissue disorders, with the hallmarks being skin hyperextensibility, joint hypermobility, and tissue fragility affecting the skin, ligaments, joints, blood vessels, and internal organs [Steinmann et al., 2002]. Dominant-negative effects or haploinsufficiency of mutant procollagen α-chain genes or deficiency of collagen-processing enzymes have been found to cause EDS [Mao and Bristow, 2001]. In a revised nosology, EDS was classified into six major types [Beighton et al., 1998] and several other forms have also been identified based on the molecular and biochemical abnormalities [Abu et al., 2008; Giunta et al., 2008; Kresse et al., 1987; Schalkwijk et al., 2001; Schwarze et al., 2004].

Homozygous or compound heterozygous *CHST14* mutations have been found in 11 patients aged 0 day to 6 years at the initial publication (from four families) with ATCS [Dündar et al., 1997, 2001, 2009; Janecke et al., 2001; Sonoda and Kouno, 2000], in six patients aged 2–32 years (from six families) with EDSKT [Kosho et al., 2005, 2010; Miyake et al., 2010; Yasui et al., 2003], and in three patients aged 12–22 years (from two families) with MCEDS [Malfait et al., 2010]. Lack of detailed clinical information from later childhood to adulthood in ATCS and lack of detailed clinical information from birth to early childhood in EDSKT and MCEDS have made it difficult to determine whether the three conditions would be distinct clinical entities or a single clinical entity with variable expressions and with different presentations depending on the patients' ages at diagnosis [Miyake et al., 2010], though the latter notion was suspected to be appropriate [Janecke et al., 2011; Malfait et al., 2010]. We, therefore, have just published an article in *American Journal of Medical Genetics Part A*, describing detailed clinical findings and courses of two additional unrelated EDSKT patients, aged 2 and 6 years, which could definitely unite the three conditions [Shimizu et al., 2011]. Furthermore, we have presented a comprehensive review of all reported patients with D4ST1 deficiency, which concludes that the three conditions constitute a clinically recognizable disorder, characterized by progressive multisystem fragility-related manifestations and various malformations and allows us to term the disorder "D4ST1-deficient EDS" [Shimizu et al., 2011]. The clinical manifestations are summarized in Table 1.

We have categorized D4ST1 deficiency into a form of EDS for substantial reasons. Clinically, the disorder satisfies all the hallmarks of EDS [Steinmann et al., 2002]. All patients we have encountered were diagnosed with EDS and have been managed as having generalized connective tissue fragility, such as preventing skin wounds, hematomas, joint dislocations, and progressive talipes and spinal deformities. Careful surgical suturing of torn skin and regular evaluations of internal organs (e.g., cardiac valve abnormalities, aortic root dilation, and bladder enlargement) and ocular abnormalities are also conducted. ATCS is surely a helpful term to detect and diagnose patients at birth, but it is indeed questionable whether the term would be appropriate for the lifelong management of patients with the disorder. Furthermore, clinical manifestations extending beyond the core features of EDS are considered not as excluding information from EDS as Janecke et al. [2011] have claimed, but as wide clinical variability in EDS such as muscle hypotonia and chronic pain in most of the types, talipes equinovarus and facial characteristics in vascular type, and congenital hip dislocation in arthrochalasia type [Beighton et al., 1998; Voermans et al., 2009].

Etiologically, multisystem fragility in D4ST1 deficiency was illustrated to be caused by impaired assembly of collagen fibrils resulting from loss of dermatan sulfate (DS) in the decorin glycosaminoglycan side chain [Miyake et al., 2010], which justifies terming the

This article was published online on 24 August 2011 as DOI.10.1002/humu.21594. In order to rectify a technical error, it has been republished on 30 September 2011 as DOI.10.1002/humu.21586.

Table 1. Clinical Manifestations in D4ST1 Deficiency

Craniofacial	*Cardiovascular*
Large fontanelle (early childhood)	Congenital heart defects (ASD)
Hypertelorism	Valve abnormalities (MVP, MR, AR, ARD)
Short and downslanting palpebral fissures	Large subcutaneous hematomas
Blue sclerae	*Gastrointestinal*
Short nose with hypoplastic columella	Constipation
Ear deformities (prominent, posteriorly rotated, low set)	Diverticula perforation
Palatal abnormalities (high, cleft)	*Respiratory*
Long philtrum and thin upper lip	(Hemo) pneumothorax
Small mouth/microretrognathia (infancy)	*Urogenital*
Slender face with protruding jaw (from school age)	Nephrolithiasis/cystolithiasis
Asymmetric face (from school age)	Hydronephrosis
Skeletal	Dilated/atonic bladder
Marfanoid habitus/slender build	Inguinal hernia
Congenital multiple contractures (fingers, wrists, hips, feet)	Cryptorchidism
Recurrent/chronic joint dislocations	Poor breast development
Pectus deformities (flat, excavated)	*Ocular*
Spinal deformities (scoliosis, kyphoscoliosis)	Strabismus
Peculiar fingers (tapering, slender, cylindrical)	Refractive errors (myopia, astigmatism)
Progressive talipes deformilies (valgus, planus, cavum)	Glaucoma/elevated intraocular pressure
Cutaneous	Microcornea/microphthalmia
Hyperextensibility/redundancy	Retinal detachment
Bruisability	*Hearing*
Fragility/atrophic scars	Hearing impairment
Fine/acrogeria-like palmar creases	*Neurological*
Hyperalgesia to pressure	Ventricular enlargement/asymmetry
Recurrent subcutaneous infections/fistula	*Development*
	Hypotonia/gross motor delay

ASD: atrial septal defect; MVP: mitral valve prolapse; MR: mitral valve regurgitation; AR: aortic valve regurgitation; ARD: aortic rot dilation.

disorder a form of EDS. However, ultrastructural findings in the skin from patients with ATCS and MCEDS were not consistent with those in patients with EDSKT, characterized by intact collagen fibrils not assembled regularly or tightly [Miyake et al., 2010]. For patients with ATCS, the skin was assessed as normal [Dündar et al., 2009]. For those with MCEDS, most collagen bundles were found to be small sized, some of which were composed of variable diameter collagen fibrils separated by irregular interfibrillar spaces [Malfait et al., 2010]. Ultrastructural and glycobiological studies on the skin from other patients as well as those on other affected tissues such as bone, muscle, and intestine would be necessary to delineate the wide spectrum of pathophysiology. Involvement of other DS-containing proteoglycans such as biglycan should also be investigated. Various malformations observed in the disorder might not simply be explained by connective tissue fragility, as they are considered to be inborn errors of development [Dündar et al., 2009; Zhang et al., 2010].

Based on the clinical, molecular, ultrastructural, and glycobiological data to date, D4ST1 deficiency is characterized by a unique set of clinical features consisting of progressive multisystem fragility-related manifestations and various malformations (Table 1). Further clinical and etiological evidences would solve the problem regarding which name should be the most appropriate: "Dermatan Sulfate-Deficient Adducted Thumb-Clubfoot Syndrome" or "D4ST1-Deficient EDS." Until then, we propose that the name "D4ST1-Deficient EDS (Adducted Thumb-Clubfoot Syndrome)" would be preferable.

References

Abu A, Frydman M, Marek D, Pras E, Nir U, Reznik-Wolf H, Pras E. 2008. Deleterious mutations in the zinc-finger 469 gene cause brittle cornea syndrome. Am J Hum Genet 82:1217–1222.

Beighton P, De Paepe A, Steinmann B, Tsipouras P, Wenstrup R. 1998. Ehlers–Danlos syndromes: revised nosology, Villefranche, 1997. Am J Med Genet 77:31–37.

Dündar M, Demiryilmaz F, Demiryilmaz I, Kumandas S, Erkilic K, Kendirch M, Tuncel M, Ozyazgan I, Tolmie JL. 1997. An autosomal recessive adducted thumb-club foot syndrome observed in Turkish cousins. Clin Genet 51:61–64.

Dündar M, Kurtoglu S, Elmas B, Demiryilmaz F, Candemir Z, Ozkul Y, Durak AC. 2001. A case with adducted thumb and club foot syndrome. Clin Dysmorphol 10:291–293.

Dündar M, Müller T, Zhang Q, Pan J, Steinmann B, Vodopiutz J, Gruber R, Sonoda T, Krabichler B, Utermann G, Baenziger JU, Zhang L, Janecke AR. 2009. Loss of dermatan-4-sulfotransferase 1 function results in adducted thumb-clubfoot syndrome. Am J Hum Genet 85:873–882.

Giunta C, Elçioglu NH, Albrecht B, Eich G, Chambaz C, Janecke A, Yeowell H, Weis MA, Eyre DR, Kraenzlin M, Steinmann B. 2008. Spondylocheiro dysplastic form of the Ehlers-Danlos syndrome-an autosomal recessive entity caused by mutations in the zinc transporter gene *SLC*39A13. Am J Hum Genet 82:1290–1305.

Janecke AR, Baenziger JU, Müller T, Dündar M. 2011. Letter to the Editors. Loss of dermatan-4-sulfotransferase 1 (D4ST1/*CHST14*) function represents the first dermatan sulfate biosynthesis defect, "Dermatan sulfate-deficient adducted thumb-clubfoot syndrome". Hum Mutat 32:484–485.

Janecke AR, Unsinn K, Kreczy A, Baldissera I, Gassner I, Neu N, Utermann G, Müller T. 2001. Adducted thumb-club foot syndrome in sibs of a consanguineous Austrian family. J Med Genet 38:265–269.

Kosho T, Miyake N, Hatamochi A, Takahashi J, Kato H, Miyahara T, Igawa Y, Yasui H, Ishida T, Ono K, Kosuda T, Inoue A, Kohyama M, Hattori T, Ohashi H, Nishimura G, Kawamura R, Wakui K, Fukushima Y, Matsumoto N. 2010. A new Ehlers–Danlos syndrome with craniofacial characteristics, multiple congenital contractures, progressive joint and skin laxity, and multisystem fragility-related manifestations. Am J Med Genet Part A 152A:1333–1346.

Kosho T, Takahashi J, Ohashi H, Nishimura G, Kato H, Fukushima Y. 2005. Ehlers–Danlos syndrome type VIB with characteristic facies, decreased curvatures of the spinal column, and joint contractures in two unrelated girls. Am J Med Genet Part A 138A:282–287.

Kresse H, Rosthoj S, Quentin E, Hollmann J, Glossl J, Okada S, Tonnesen T. 1987. Glycosaminoglycan-free small proteoglycan core protein is secreted by fibroblasts from a patient with a syndrome resembling progeroid. Am J Hum Genet 41:436–453.

Malfait F, Syx D, Vlummens P, Symoens S, Nampoothiri S, Hermanns-Lê, Van Lear L, De Paepe A. Musculocontractural Ehlers–Danlos syndrome (former EDS type VIB) and adducted thumb clubfoot syndrome (ATCS) represent a single clinical entity caused by mutations in the dermatan-4-sulfotransferase 1 encoding *CHST14* gene. 2010. Hum Mutat 31:1233–1239.

Mao JR, Bristow J. 2001. The Ehlers–Danlos syndrome: on beyond collagens. J Clin Invest 107:1063–1069.

Miyake N, Kosho T, Mizumoto S, Furuichi T, Hatamochi A, Nagashima Y, Arai E, Takahashi K, Kawamura R, Wakui K, Takahashi J, Kato H, Yasui H, Ishida T, Ohashi H, Nishimura G, Shiina M, Saitsu H, Tsurusaki Y, Doi H, Fukushima Y, Ikegawa S, Yamada S, Sugahara K. Matsumoto N. 2010. Loss-of-function mutations of *CHST14* in a new type of Ehles–Danlos syndrome. Hum Mutat 31:966–974.

Schalkwijk J, Zweers MC, Steijlen PM, Dean WB, Taylor G, van Vlijmen IM, van Haren B, Miller WL, Bristow J. 2001. A recessive form of the Ehlers-Danlos syndrome caused by tenascin-X deficiency. N Engl J Med 345:1167–1175.

Schwarze U, Hata R, McKusick VA, Shinkai H, Hoyme HE, Pyeritz RE, Byers PH. 2004. Rare autosomal recessive cardiac valvular form of Ehlers-Danlos syndrome results from mutations in the COL1A2 gene that activate the nonsense-mediated RNA decay pathway. Am J Hum Genet 74:917–930.

Shimizu K, Okamoto N, Miyake N, Taira K, Sato Y, Matsuda K, Akimaru N, Ohashi H, Wakui K, Fukushima Y, Matsumoto N, Kosho T. 2011. Delineation of dermatan 4-O-sulfotransferase 1 deficient Ehlers-Danlos syndrome: observation of two additional patients and comprehensive review of 20 reported patients. Am J Med Genet Part A 155A:1949–1958.

Sonoda T, Kouno K. 2000. Two brothers with distal arthrogryposis, peculiar facial appearance, cleft palate, short stature, hydronephrosis, retentio testis, and normal intelligence: a new type of distal arthrogryposis? Am J Med Genet 91:280–285.

Steinmann B, Royce PM, Superti-Furga A. 2002. The Ehlers–Danlos syndrome. In: Royce PM, Steinmann B, editors. Connective tissue and its heritable disorders. New York: Wiley-Liss. p 431–523.

Voermans, NC, van Alfen N, Pillen S, Lammens M, Schalkwijk J, Zwarts MJ, van Rooij IA, Hamel BCJ, van Engelen BG. 2009. Neuromuscular involvement in various types of Ehlers–Danlos syndrome. Ann Neurol 65:687–697.

Yasui H, Adachi Y, Minami T, Ishida T, Kato Y, Imai K. 2003. Combination therapy of DDAVP and conjugated estrogens for a recurrent large subcutaneous hematoma in Ehlers–Danlos syndrome. Am J Hematol 72:71–72.

Zhang L, Müller T, Baenziger JU, Janecke AR. 2010. Congenital disorders of glycosylation with emphasis on loss of dermatan-4-sulfotransferase? 93:289–307.

Tomoki Kosho,[1]* Noriko Miyake,[2] Shuji Mizumoto,[3] Atsushi Hatamochi,[4] Yoshimitsu Fukushima,[1] Shuhei Yamada,[3] Kazuyuki Sugahara,[3] and Naomichi Matsumoto[2]

[1]Department of Medical Genetics, Shinshu University School of Medicine, Matsumoto, Japan; [2]Department of Human Genetics, Yokohama City University Graduate School of Medicine, Yokohama, Japan; [3]Laboratory of Proteoglycan Signaling and Therapeutics, Hokkaido University Graduate School of Life Science, Sapporo, Japan; [4]Department of Dermatology, Dokkyo Medical University, School of Medicine, Mibu, Japan

*Correspondence to: Tomoki Kosho, Department of Medical Genetics, Shinshu University School of Medicine, 3-1-1 Asahi, Matsumoto 390-8621, Japan. E-mail: ktomoki@shinshu-u.ac.jp

Received 9 April 2011; accepted revised manuscript 3 August 2011.
DOI: 10.1002/humu.21586, Published online 24 August 2011 in Wiley Online Library (www.wiley.com/humanmutation).